Theor. Appl. Climatol. 51, 25–38 (1995)

Theoretical and Applied Climatology

© Springer-Verlag 1995
Printed in Austria

[1] Laboratory of Climatology, Department of Physical Geography, Earth Sciences Centre, Göteborgs University, Sweden
[2] Physics II, Alfred-Wegener-Institute for Polar and Marine Research, Bremerhafen, Germany

A 1-D Atmospheric Energy Balance Model Developed for Ocean Modelling

D. Chen[1], R. Gerdes[2], and G. Lohmann[2]

With 9 Figures

Received August 15, 1994

Summary

We present a simple, deterministic energy balance model. The model is designed to represent the atmospheric component of the coupled atmosphere-ocean system. It is a one dimensional, global model with time and space resolutions of one year and 10° of latitude respectively. The model predicts the surface air temperature and estimates the surface freshwater flux diagnostically. The coupling between the atmospheric model and an ocean model is accomplished by heat and freshwater fluxes at their interface. The heat flux is calculated according to the difference in the surface air temperature and ocean surface temperature, while the freshwater flux is estimated from the latent heat transport in the atmosphere by a diagnostic equation. Two parameterizations for the latent heat transport are proposed, which distinguishes the two versions of the model.

Before proceeding with interactive runs, we study the behaviour of the model in a decoupled mode. Some experiments with initial conditions altered and external forcings changed are carried out to investigate the sensitivity and stability of the model. In particular, the influence of the ice-albedo feedback on model solutions is examined. The results of these experiments may be helpful both in understanding the characteristics of the model and in interpreting results when the model is coupled to an OGCM.

1. Introduction

The ocean circulation is forced by heat, momentum and freshwater fluxes at the upper boundary – the ocean surface. These fluxes provide a means for the ocean to communicate with the atmosphere. On the other hand, the atmosphere is also affected by the ocean state through the interfacial fluxes. For ocean general circulation models (OGCMs) these fluxes must be specified. There are usually two kinds of options to specify these fluxes for an OGCM. The first one is in a coupled mode; i.e. the OGCM will be coupled to an atmospheric general circulation model (AGCM) through the fluxes, like what is happening in the real world. The second one is in a decoupled mode, which means that the OGCM is forced either by some specified fluxes or by fluxes which are determined from the ocean state predicted by the ocean model and a specified atmospheric state. In this case, the atmosphere will not be influenced by the ocean. Naturally it is ideal to use the coupled mode. However, since a huge amount of computing time is needed both by OGCMs and AGCMs, this kind of coupling is simply too expensive to run. Moreover, as an OGCM is already complicated enough, adding an AGCM may make the interpretation and understanding of a coupled model much more difficult.

In the decoupled mode, climatological data for the atmosphere are used to specify the fluxes. This method has the advantage in that one only needs to deal with the ocean physics. It is simple and practical, thereby making the method the most widely used one in ocean modelling. However, it should be noted that the lack of communication between the atmosphere and the ocean is

artificial and may cause problems. It is well established that the thermohaline circulation is sensitive to specified boundary conditions such as heat flux and fresh water flux. This is especially true for the fresh water flux. A well known example of the problems in the decoupled mode is the "polar halocline catastrophe (PHC)", a term coined by F. Bryan (1986). PHCs are observed in models which use mixed boundary conditions. These models are forced by a specified fresh water flux and a relaxation of the surface temperature to a specified value. The fresh water flux is usually diagnosed from an equilibrium run in which the ocean model is spun up by restoring boundary conditions both on surface temperature and salinity. Most studies (e.g., Weaver et al., 1993) emphasise the influence of the specified fresh water flux on the collapse of the thermohaline circulation, while a few studies also touch the possible effects of the heat flux. Recently, Zhang et al. (1993) investigated the effects of the heat flux associated with the mixed boundary conditions. They point out that the fixed atmospheric temperature is also responsible for the occurrence of a PHC. When the atmospheric temperature is allowed to response to the heat flux in such a way that the heat capacity of the atmosphere is set to be zero, they find that a PHC is less likely to occur. This result demonstrates the necessity of including a simple atmospheric component to improve the boundary conditions for the ocean model.

As the two mentioned modes have their own difficulties, it turns out that we ought to seek an intermediate method to overcome the difficulties. This method, on one side, should allow some communication between the atmosphere and the ocean; and on the other side, the atmospheric component should be so simple that only a small amount of additional computer time is needed. We intend here to develop an atmospheric model which is simple enough to be tractable but still has the essential physics that is relevant to the problem. Energy balance models appear to meet these requirements. To start with, we develop a one dimensional EBM which has the ability to predict surface air temperature and to diagnose the fresh water flux. It is hoped that the coupling of this EBM to an OGCM will help to establish an intermediate way to study long term change in coupled ocean-atmosphere system.

We shall first formulate the atmospheric model and the coupling between the atmospheric model and ocean model in Section 2. Then, a description of all parameterizations is given in Section 3. Section 4 explaines the tuning procedure of the model. In order to identify the model stability and sensitivity, some experiments with regard to different perturbations and the parameterization schemes used by the model are carried out in Section 5. At last, a summary of the results can be found in Section 6.

2. Formulation of the Coupled System

2.1 Governing Equation of the Atmospheric Model

The vertically and zonally averaged thermodynamic equation of the atmosphere, averaged over one year may be written as

$$\frac{1}{g}\int_0^{p_0}\left[C_p\frac{\partial \bar{T}}{\partial t}\right]dp = [\bar{R}_t] - [\bar{R}_b] + L[\bar{P}] + [\bar{S}\bar{H}] - \frac{1}{g}\int_0^{p_0}\operatorname{div}[\bar{F}_s]dp \qquad (1)$$

where $C_p(\mathrm{Jkg^{-1}K^{-1}})$ is the specific heat at constant pressure, T(K) atmospheric temperature, t(s) time, p(mb) the pressure, R_t and $R_b(\mathrm{Wm^{-2}})$ downward net radiative fluxes at the top ($p=0$) and the bottom ($p=p_0$) of the atmosphere, $L(\mathrm{Jkg^{-1}})$ the latent heat of vaporization and P precipitation ($\mathrm{kgm^{-2}s^{-1}}$), $SH(\mathrm{Wm^{-2}})$ the sensible heat released from the ground to the atmosphere, and $\frac{1}{g}\int_0^{p_0}\operatorname{div}[\bar{F}_s]dp(\mathrm{Wm^{-2}})$ is divergence of vertically integrated sensible heat flux in the atmosphere. An overbar and a bracket have been used to denote the zonal mean and time mean operators respectively. Similarly the conservation of water vapour in the atmosphere may be written as

$$L([\bar{E}] - [\bar{P}]) - \frac{1}{g}\int_0^{p_0}\operatorname{div}[\bar{F}_l]dp = 0 \qquad (2)$$

where $\frac{1}{g}\int_0^{p_0}\operatorname{div}[\bar{F}_l]dp$ is divergence of vertically integrated latent heat flux in the atmosphere ($\mathrm{Wm^{-2}}$).

For the sake of simplicity, all overbars and brackets will subsequently be dropped. Substituting (2) into (1), we arrive at the governing equation for the atmospheric model:

$$\frac{1}{g}\int_0^{p_0} C_p\frac{\partial T}{\partial t}dp = -\frac{1}{g}\int_0^{p_0}\operatorname{div}F_s dp - \frac{1}{g}\int_0^{p_0}\operatorname{div}F_l dp + R_t - F_{oa} \qquad (3)$$

where $F_{oa}(\mathrm{Wm}^{-2})$ is the sum of all downward heat fluxes at the surface. Note that the annual average of F_{oa} vanishes over land surfaces, so it is the heat exchange between the atmosphere and ocean that accounts for F_{oa}. If a subscript o denotes ocean surface, and f_o is the fraction of area covered by ocean in a latitude zone, we have

$$F_{oa} = f_o(R_{so} - SH_o - LE_o). \tag{4}$$

2.2 Coupling Between the Atmosphere and Ocean

To illustrate the coupling between the atmosphere and ocean represented by the derived atmospheric model and an OGCM, we need a simplified equation to represent the ocean model. The vertically integrated energy balance equation for the ocean may be written as

$$ST_o = F_{oa} - \int_H \mathrm{div}\, F_o dz \tag{5}$$

where $ST_o(Wm^{-2})$ is the vertically integrated heat storage in the ocean due to a change in temperature, and $\int_H \mathrm{div}\, F_o dz\,(\mathrm{Wm}^{-1})$ is the vertically integrated sensible heat divergence in the ocean. Equation (5) gives rise to the first coupling between the model atmosphere and model ocean through heat fluxes at their interface. Following Haney (1971), the sum of all interfacial heat fluxes can be parameterized in terms of the difference in surface air temperature and ocean surface temperature (SST),

$$R_{so} - SH_o - LE_o = \frac{C_{po}\rho_o D}{\tau}(T_0 - SST) \tag{6}$$

where C_{po} is the specific heat of sea water, ρ_o the density of top layer water, D the depth of the top layer of the ocean model, and τ the time constant which is chosen to be 30 days.

The second coupling of the two components is through the freshwater flux at the ocean surface. This flux is approximately related to the virtual salt flux Q_s^* at the ocean's surface by

$$P - E = \frac{L\rho_*}{S_*} Q_s^* \tag{7}$$

where ρ_* and S_* are reference density and salinity of the sea water.

3. Parameterizations

3.1 Relationship Between the Vertically Integrated Temperature and the Surface Air Temperature

As we are interested in the coupling between the atmosphere and ocean, the air temperature at the sea level rather than the vertically integrated temperature would be directly relevant. Therefore, we need to establish the relationship between the vertically integrated temperature and the surface air temperature. Rennick (1977) analysed the data from Oort and Rasmusson (1971) and Taljaard et al. (1969), and concluded that the local vertical gradients of the zonally averaged potential temperature at different levels are essentially constant, although they vary with latitude. Based on this finding, temperature at any given altitude in the troposphere may be expressed as a function of

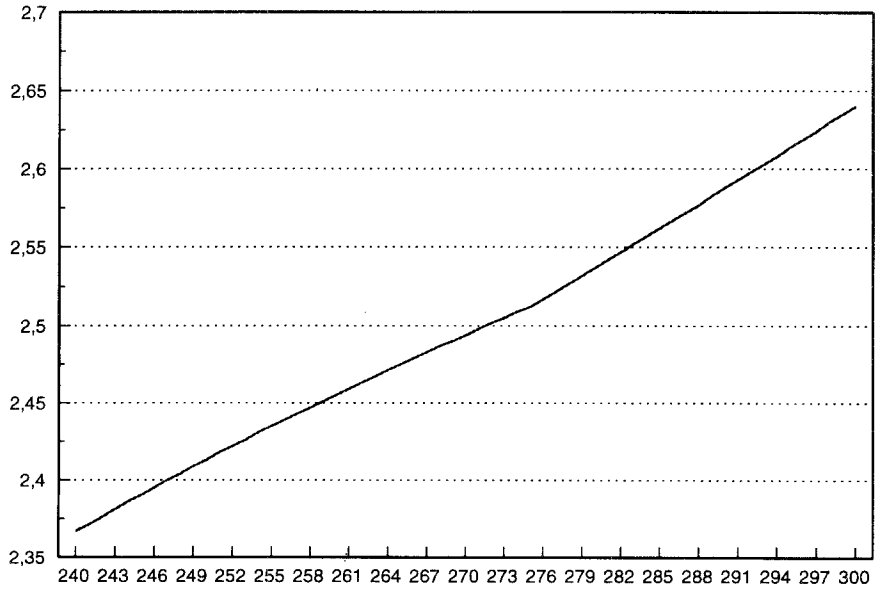

Fig. 1. The relationship between the vertically integrated temperature and the surface temperature. The horizontal coordinate represents the surface air temperature T_0 in K, whereas the vertical coordinate shows the vertically integrated temperature $\frac{1}{g}\int_0^{p_0} T dp$ in $10^6\,\mathrm{K\,kgm}^{-2}$

surface air temperature and the vertical gradient of the atmospheric potential temperature at a particular latitude. From Eqs. (3) through (8) given in Rennick's paper, we can calculate the vertically integrated temperature as a function of the surface air temperature. The result is shown in Fig. 1. There is a nearly linear relation between the two temperatures. However, closer inspection of the curve reveals that the curve can be much better represented by two straight lines with different slopes instead of one straight line. The two lines join together at about 275 K. For the present climate, this temperature is observed at about $50° \frac{S}{N}$. Thus it is concluded that two distinct linear relationships exist for low-middle latitudes and high latitudes. These relationships can be fairly well repesented by the following equations:

$$\frac{1}{g}\int_0^{p_0} \frac{\partial T}{\partial t}\, dp = \beta \frac{\partial T_0}{\partial t}; \tag{8}$$

and

$$\beta = \begin{cases} 5708\,\mathrm{kg\,m^{-2}} & \text{for} \quad T_0 \geqslant 275\,\mathrm{K} \\ 3966\,\mathrm{kg\,m^{-2}} & \text{for} \quad T_0 < 275\,\mathrm{K}. \end{cases} \tag{9}$$

One-layer EBMs have to deal with the problem of relating the surface air temperature to the vertically averaged temperature. This result is interesting for such a simple EBM because it shows that the surface air temperature can be related to the vertically averaged temperature through two constants globally. The usual assumption made with one-layer EBM so far is that the two temperatures can be related to each other with a single constant globally. Unfortunately, this assumption comes neither from theoretical reasoning nor from empirical estimation. The single constant used by many EBMs are therefore more or less arbitrary. This calculation may provide an empirical means to estimate the single constant used by many time dependent EBMs. As indicated by the result, should just one constant be used for the global atmosphere, the best choice would be $5300\,\mathrm{kg\,m^{-2}}$. Actually, from the unit of β we can see that βC_p can be interpreted as thermal inertia ($\mathrm{Jm^{-2}\,K^{-1}}$) of a column of air. The constant β is written as $\rho_a H_a$ in some EBMs. Here ρ_a and H_a are surface air density and an effective atmosphere height, respectively. For example, Stocker et al. (1992) specify $\rho_a = 1.225\,\mathrm{kg\,m^{-3}}$ and $H_a = 8320$ m. According to our result, H_a should be equal to 4327 m if the same density is used. Thus, the two different constants found in this study simply represent the two different heat capacities of the air column in two different latitude-zones as it is 'felt' by the surface air temperature. As the density does not change so much, this implies that the difference exists mainly in the effective height of the atmosphere.

It is also worth noting that the heat capacity of the air column determines the time scale of the atmospheric thermal response to forcings in general case while it is a dummy variable in the equilibrium state. This can explain the astonishing success of simple EBMs in simulating equilibrium climate states. It is desirable, however, that the constants be determined on the sound basis when we are to study the interaction between the atmosphere and ocean.

3.2 Net Radiative Flux at the Top of the Atmosphere

The net radiative flux at the top of the atmosphere can be expressed by

$$R_t = Q(1 - \alpha_p) - I \tag{10}$$

where Q is the extraterrestrial insolation, α_p is the planetary albedo, and I is the outgoing infrared radiation.

The incoming solar radiation is calculated by

$$Q = S_0 \mu \tag{11}$$

where $S_0 = 1376\,\mathrm{Wm^{-2}}$ is the solar constant, and μ is an annual averaged cosine zenith angle multiplied by fractional daylight time, which is calculated by the 5th order polynomial given by Roads and Vallis (1984).

Following Sellers (1969), α_p is made a function of the surface air temperature and latitude,

$$\alpha_p = \begin{cases} b(\phi) + f T_0 & \text{for } T_0 < 283\,\mathrm{K} \\ \alpha_p^o & \text{for } T_0 \geqslant 283\,\mathrm{K} \end{cases} \tag{12}$$

where α_p^o is the observed planetary albedo for the present climate, $f = \partial \alpha_p / \partial T_0$ is the so called ice-albedo feedback factor which is a measure of the strength of the ice-albedo feedbackand, and b is a latitude-dependent constant. As we believe that this parameter is important for the model sensitivity, we will vary f to study effect of this parameter. Once f is chosen, b is calculated by matching the estimated α_p to α_p^o using the observed temperature at a latitude zone. Through the introduction of f the parameterization incorporates in a sample

way the adjustable positive feedback due to high albedo of snow and sea ice.

The outgoing long wave radiation is estimated using the parameterization proposed by Budyko (1969),

$$I = A + BT_0 \tag{13}$$

where A and B are empirical constants.

3.3 Meridional Heat Transport

Version one: Manabe and Bryan (1985) have studied the heat transport in the atmosphere and the ocean under different CO_2 forcings using a coupled AGCM and OGCM. They find that the total heat transport by the combined system is relatively insensitive to different atmospheric CO_2 concentrations ranging from 150 ppm to 2400 ppm. This is particularly true for the range of 300 ppm to 2400 ppm. This is due to the negligible change in intensity of the thermohaline circulation in the model ocean and the compensation in changes of sensible and latent heat transport in the atmosphere. Based on this finding, the total heat transport will be kept at its present climatological value. In this way, the atmospheric heat transport can be determined by subtracting the oceanic transport from the specified total transport. In order to estimate the precipitation minus evaporation rate, however, we need to know the latent heat transport. As the sensible heat transport is more readily related to the meridional gradient of the surface air temperature, we parameterize it as

$$\frac{1}{g}\int_0^{p_0} F_s dp = -K_s \frac{\partial T_0}{\partial y} \tag{14}$$

where $K_s(\mathrm{WK}^{-1})$ is diffusion coefficient for the atmospheric sensible heat. It will be determined by fitting the related climatological data and be kept constant. The evaporation minus precipitation rate will be diagnostically computed from the latent heat transport by (2). Obviously the determination of the latent heat transport is essential to the estimation of the freshwater flux. For that reason we would like to try the second parameterization for the heat transport in order to test the influence of the transport schemes on the freshwater flux. By studying the performances of the schemes it may be possible to judge which one is more appropriate for the formulation of the coupled system.

Version two: The second parameterization is different from the first one in that the total heat transport is no longer invariant. Thus we need to parameterize the sensible and latent heat transport in the atmosphere separately. However, the two fluxes are not totally independent. Actually, both of them are related to the meridional gradient of the surface air temperature. If we assume that the flux of moisture can be approximated by a diffusion process, the latent heat flux may be parameterized as

$$\frac{1}{g}\int_0^{p_0} F_l dp = -K_l \frac{L}{C_p}\frac{\partial q_0}{\partial y} \tag{15}$$

where $K_l(\mathrm{WK}^{-1})$ is the diffusion coefficient for the water vapour and q_0 is the mixing ratio of surface air humidity. This is based on the fact that water vapor is concentrated near the surface. q_0 can be related to surface temperature through the relative humidity RH by the following equation:

$$q_0 = q_{0s}(T_0)RH \tag{16}$$

where q_{0s} is the surface saturation mixing ratio.

If we make a further assumption that RH remains constant, we can rewrite (15) as

$$\frac{1}{g}\int_0^{p_0} F_l dp = -K_l \frac{L}{C_p} RH \frac{\partial q_{0s}}{\partial T_0}\frac{\partial T_0}{\partial y}. \tag{17}$$

4. Tuning Procedure

In calibrating the model parameterizations, the satellite data of outgoing radiation, net radiation and planetary albedo from Stephens et al. (1981), surface air temperature from Oort (1983), and latent heat transport from Sellers (1969) will be used. It should be kept in mind that these data are not averaged over the same period of time and there may be errors in them. Furthermore, the length of observational records may not be long enough to be representative for an equilibrium state of the atmosphere-ocean system. Therefore, these data will be checked against the governing equations and will be manipulated, if necessary, so that they will obey the model physics.

4.1 Total Heat Transport

Adding (5) into (3) and assuming the coupled ocean-atmosphere is in equilibrium, we have

$$\frac{1}{g}\int_0^{p_0} \mathrm{div}(F_l + F_s)dp + \int_H \mathrm{div}\, F_o dz = R_t \tag{18}$$

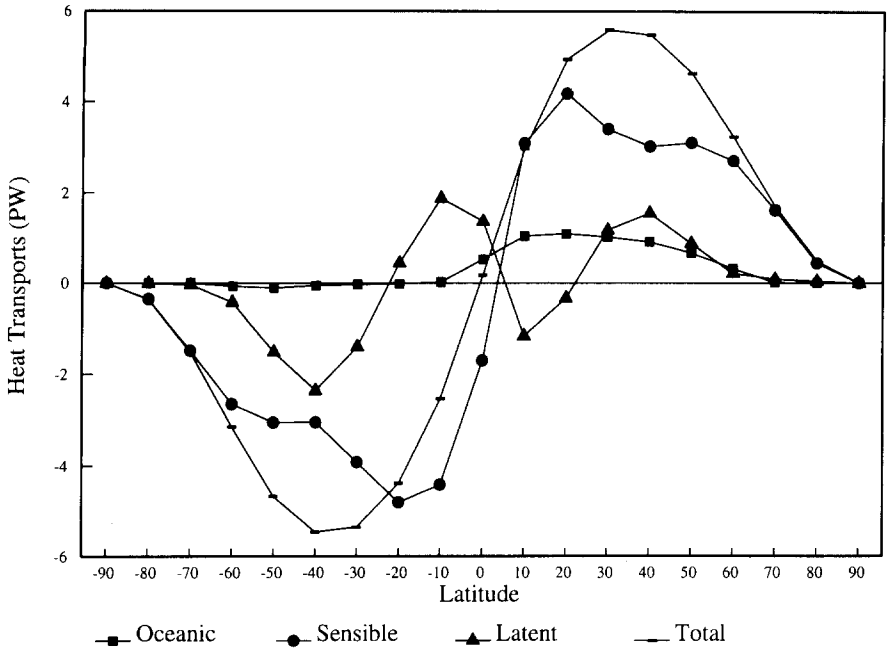

Fig. 2. Components of the heat transport in the combined system: The total transport is estimated using the net radiation flux data from Stephens et al., the latent transport is from Sellers, the oceanic transport is from an equilibrium run of our global ocean model, and the sensible transport is calculated as a residual the total transport from all other components

By integrating (18) with the observed radiation balance, we should be able to get the total northward heat transport in the coupled atmosphere-ocean system. However, the globally integrated heat divergence implied by the radiation data is not zero. The simplest way to overcome this difficulty is to subtract the global mean from the original radiation data at each latitude zone and use this 'corrected' value of R_t. The total heat transport calculated in this way is displayed in Fig. 2. The transport compares favourably with the estimate by Carissimo et al. (1985) and others (not shown).

4.2 Outgoing Longwave Radiation

The original data has been modified to meet the requirements of (18). We choose to correct the outgoing radiation data simply because of its relatively great magnitude. The modified outgoing radiation and the temperature data are used to estimate A and B in (13). A linear correlation shows that $A = 213.35\,\mathrm{Wm}^{-2}$ and $B = 2.22\,\mathrm{Wm}^{-2}\mathrm{K}^{-1}$. The correlation coefficient is 0.98.

4.3 Diffusion Coefficients

We need first to compute the oceanic transport before we can estimate the atmospheric transport and the related diffusion coefficients. For that purpose we use an OGCM which will be coupled to the EBM. The OGCM is the GFDL code known as mom. (Pacanowski et al., 1991). The ocean model extends from 66° S to 80° N in latitude and from 60° W to 14° E in longitude. Thus it has only a single basin with a width of 74° of longitude. The horizontal resolution of the model is 2° × 2°, while in the vertical it has 15 levels. The depth of the ocean is 5700 m everywhere. For the sake of greatest possible consistency, the ocean model is forced by the atmospheric temperature from Oort and a prescribed surface salinity through Newtonian damping terms acting at the uppermost level. The ocean model is integrated until equilibrium is reached. Then the longitudinally averaged heat transport is computed. The result is displayed in Fig. 2.

Now we turn to the question of how to divide the atmospheric transport into latent and sensible transport. We found if we use the sensible heat flux from Sellers, we will get a much higher latent heat transport since the oceanic transport from Sellers is much larger than that of our ocean model. Considering the importance of the latent heat transport for the freshwater flux determination, we chose to use the latent heat flux of Sellers plus the estimated oceanic transport and the specified total transport to calculate the sensible heat flux as a residual. Then we will use this adjusted flux to compute the diffusion coefficient. The adjusted sensible heat flux, along with the

latent and the total heat transport used, is also displayed in Fig. 2. We see that the maximum value of the sensible heat flux is about ± 4.5 PW (1 PW $= 10^{15}$ W) which is somewhat (about 1.5 PW) greater than those estimated by radiosonde observations. However, it is found that AGCM simulations usually have significant greater value of atmospheric transport than indicated from the radiosonde observations, which is argued by Covey (1988) to be more closer to the truth. It should also be pointed out that since the climatology of the sensible heat transport is estimated as a residual, its value may include errors in all involved terms.

The latitudinal profile of the diffusion coefficient for the sensible heat calculated in this way is shown in Fig. 3. Note that $K_s/\beta C_p$ rather than K_s is displayed. It is seen that the coefficient varies from $10^5\,m^2s^{-1}$ to $10^7\,m^2s^{-1}$. The diffusion coefficient peeks at equator, which can be explained by the very small meridional temperature gradient there. The almost evenly distributed diffusion coefficient in middle and high latitudes may be an indication that the transport processes there may be well approximated by a diffusion process.

For the second version, the diffusion coefficient for the latent heat also needs to be determined. Using the climatology of the temperature and the latent heat flux, the diffusion coefficient for water vapour is calculated and shown in Fig. 3. In the calculation the relative humidity RH is taken as 0.8 everywhere. Also, $K_l/\beta C_p$ rather than K_l is displayed. The diffusion coefficient for the latent heat transport has the same order of magnitude as those for the sensible heat transport in the extratropics. Negative values appear in the tropics, as is also found by Ghil (1976) and Harvey (1988).

4.4 *Consistent Factor*

At this stage, it is found that when the model is run using the parameterizations calibrated, we can not yet get the observed temperature distribution. This is not surprising since the model temperature is strongly determined by the outgoing radiation. As there is still 5 per cent of the radiation variation not explained by the linear parameterization (13), the predicted temperature will be affected by the error in that part of the radiation. Considering that clouds and other parameters like lapse rate which influence the outgoing radiation are not variables of the model, including these factors does not add any freedom to the model. We could, however, add a tuneable parameter to the parameterization. The parameter should take into account the effect of all unknown factors. So we have

$$I = CF(A + BT_0) \tag{19}$$

where CF is a tuneable parameter and is called 'consistent factor' by Schneider (1973). CF is estimated from the parameterization for the outgoing radiation and the temperature from Oort. It is found that CF varies between 0.94–1.07, which is considered to be relatively small. In the

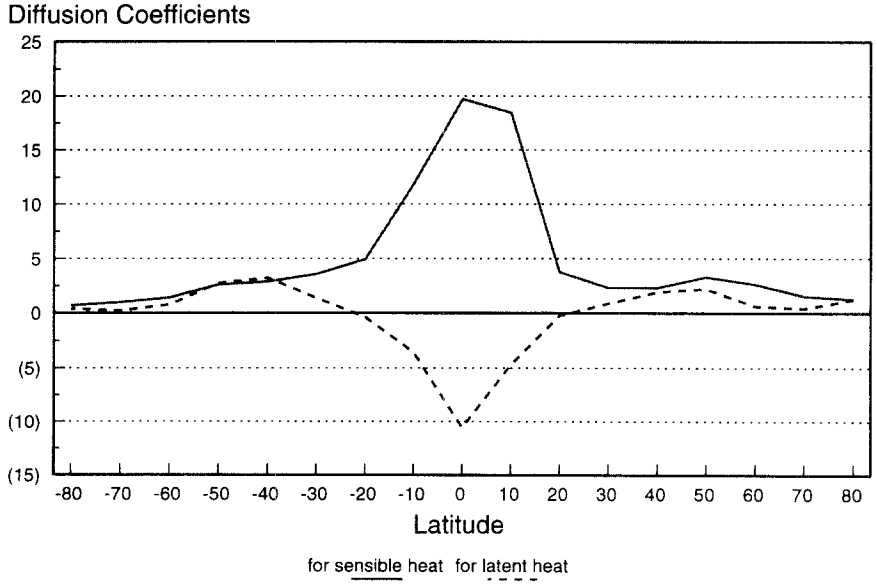

Fig. 3. Latitudinal distribution of the diffusion coefficients for the sensible ($K_s/\beta C_p$) and the latent ($K_l/\beta C_p$) heat transports in the atmosphere. Note that the later one is used only in the second version of the atmospheric model that calculates the latent heat transport explicitly. The unit of the diffusion coefficients is $10^6\,m^2s^{-1}$

model we will use (19) instead of (13) to calculate the outgoing radiation.

5. Experiments

In the preceding section the atmospheric model has been tuned completely to reproduce present climatologies of surface air temperature and freshwater flux. The consistent climatologies of the climate system will be referred to as the control climate to which solutions from other experiments will be compared. Note also that in all experiments to be described the oceanic heat transport for the control climate will be used.

The governing equation is treated as an initial-value problem with boundary conditions that the heat transport vanishes at the poles. The meridional grid spacing is chosen to be 10° of latitude from pole to pole. An explicit scheme which is forward in time and centered in space is used to solve the equation numerically. The diagnostic equation for the freshwater flux is solved with centred space differences for the meridional temperature gradient.

5.1 Version 1

We shall examine the model sensitivity of version 1 under an external perturbation of an uniform increase in net radiation of $+4\,\mathrm{Wm}^{-2}$. Such an increase is characteristic of the global warming due to a doubling of the atmospheric CO_2 (Lal and Ramanathan, 1984). The integrations with different ice-albedo feedback factors f are started with the control climate as initial condition. Figure 4 shows the changes in the temperature of the equilibrium response of the model to the perturbation with six selected ice-albedo feedback factors ranging from 0 to 0.010. It is seen that the main difference among all the experiments appears in middle and high latitudes, ranging from $40^{\circ}{}^{S}_{N}$ to $60^{\circ}{}^{S}_{N}$. The maximum increase occurs at about $50^{\circ}{}^{S}_{N}$ where the ice-albedo feedback seems to be most efficient. The almost uniform increase in the tropics is due to the parameterization of the albedo that eliminates the feedback at temperatures above 283 K. The relatively small sensitivity polarward of around $75^{\circ}{}^{S}_{N}$ can be explained by high albedos and small insolation there. Since the atmospheric heat transport is fixed, local temperature change is solely determined by change in net radiation which is associated with the ice-albedo effect. So a change of the temperature in a latitude zone is simply local, having no influence on the temperature change in another latitude zone. It is also shown by Fig. 4 that the greater f is, the stronger the increase in temperature in middle and high latitudes will be.

To choose an appropriate value of f for the model, we take a look at some similar experiments carried out with AGCMs. The increases in global mean temperature of our model are 1.8, 2.0, 2.2, 2.7, 3.2, 3.8 K for $f = 0$, 0.002, 0.004, 0.006, 0.008,

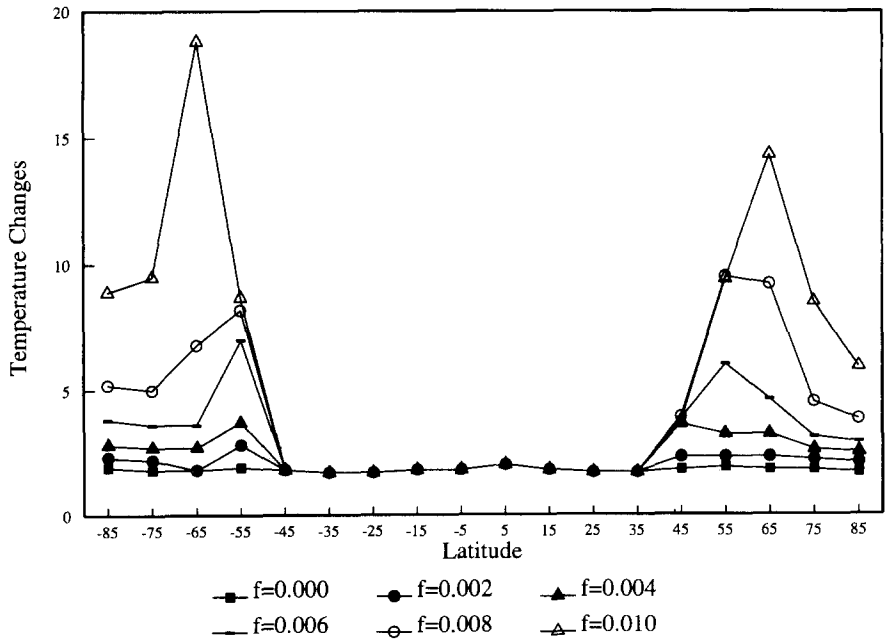

Fig. 4. Model responses to a doubling of CO_2 with different ice-albedo feedback factors. Temperature changes are expressed by the difference between equilibrium temperature distribution due to the doubling of CO_2 and that of the control climate in K

0.010 respectively, whereas AGCMs predict an increase ranging from 1.3 to 7 K (Dickinson, 1986) with a most likely range of 1.4–4.4 K (Mitchell, 1989). This implies that $f = 0.04$–0.006 seems to be a good choice for the model to produce a comparable global sensitivity to most AGCMs. However, caution must be taken when comparing results from AGCMs to that of the EBM since additional feedback mechanisms exist in AGCMs. Thus, we believe that it is necessary to isolate the ice-albedo effect in AGCMs for an approximate comparison with the EBM with regard to the feedback strength.

To discuss the global sensitivity of different climate models to external perturbations, a globally averaged model is usually used to access feedbacks qualitatively (see e.g. Lashof, 1989). This model is formulated as follows:

$$C\frac{\partial(\Delta T_0)}{\partial t} + \lambda(\Delta T_0) = \Delta R_t \tag{20}$$

where C is the heat capacity of the climate system, ΔT_0 is the change in global mean surface air temperature, ΔR_t is an externally prescribed change in net radiation, and λ is the feedback parameter of the internal dynamics of the system. As we are only concerned with the equilibrium response, (20) can be further simplified,

$$\Delta T_0 = \frac{\Delta R_t}{\lambda}. \tag{21}$$

As pointed out by Dickinson (1986), λ is an overall climate system sensitivity factor which includes the sum of all contributing feedback factors which are operative in the system. λ is a convenient measure of the strength of individual feedbacks because of its additive nature. It is possible, by carrying out experiments with certain feedbacks switched on or off, to identify individual feedback parameters due to different mechanisms. To assess the ice-albedo feedback in the model, we first estimate a reference value (λ_0) for a case without the feedback ($f = 0$). The global temperature increase in the CO_2 doubling experiment with $\Delta R_t = 4\,\mathrm{Wm}^{-2}$ is 1.8 K, implying from (21) that $\lambda_0 = 2.22$. Note that λ_0 includes black-body (λ_B) and long-wave water vapour feedbacks (λ_W). λ_B can be estimated by

$$\lambda_B = 4\sigma T_e^3 = 3.75\,\mathrm{Wm}^{-1}\,\mathrm{K}^{-1} \tag{22}$$

where $\sigma = 5.67 \times 10^{-8}\,\mathrm{Wm}^{-2}\,\mathrm{K}^{-4}$ is the Stefan-Boltzmann constant, and $T_e = 255$ K is the earth's effective radiative temperature. Then,

$$\lambda_W = \lambda_0 - \lambda_B = -1.53\,\mathrm{Wm}^{-2}\,\mathrm{K}^{-1}. \tag{23}$$

Mitchell (1987) has estimated λ_W from CO_2 doubling experiments using both radiative-convective models and AGCMs. These experiments indicate that λ_W range from $-1.4\,\mathrm{Wm}^{-2}\,\mathrm{K}^{-1}$ to $-1.8\,\mathrm{Wm}^{-2}\,\mathrm{K}^{-1}$, which agrees well with the above result.

With help of λ_0 we can estimate the contribution of the ice-albedo feedback (λ_α) to the total feedback parameter λ with different feedback factors f in our model. It is found that λ_α range from $-0.22\,\mathrm{Wm}^{-2}\,\mathrm{K}^{-1}$ to $-1.17\,\mathrm{Wm}^{-2}\,\mathrm{K}^{-1}$ as f varies from 0.002 to 0.010.

One dimensional EBMs developed so far show λ_α ranging from $-0.3\,\mathrm{Wm}^{-2}\,\mathrm{K}^{-1}$ (Lian and Cess, 1977) to $-0.8\,\mathrm{Wm}^{-2}\,\mathrm{K}^{-1}$ (Sellers, 1969), while AGCMs have an even wider range of the feedback parameter. For example, an experiment carried out by Washington and Meehl (1983) indicates $\lambda_\alpha \approx 0.0\,\mathrm{Wm}^{-2}\,\mathrm{K}^{-1}$, whereas in another experiment they found $\lambda_\alpha \approx -0.9\,\mathrm{Wm}^{-2}\,\mathrm{K}^{-1}$ (Washington and Meehl, 1984). With an interactive ocean, Spelman and Manabe (1984) find $\lambda_\alpha \approx -0.45\,\mathrm{Wm}^{-2}\,\mathrm{K}^{-1}$ which is somehow a representative value for many AGCM experiments (Mitchell, 1989).

Because the feedback parameter depends very much on sea ice and we will couple this model to an OGCM, we chose $f = 0.004$, which corresponds to $\lambda_\alpha \approx -0.40\,\mathrm{Wm}^{-2}\,\mathrm{K}^{-1}$. Another reason why we prefer a small value of f in version 1 is that it produces too strong local sensitivity at middle latitudes.

To investigate the effect of the feedback factor on stability, we first carried out some time integrations from initial conditions close to the control climate state. Time-dependent solutions of the initial-value problem will converge as $t \to \infty$ to a steady state which is near the control climate if it is stable. The results show that solutions converge with perturbations as large as ± 10 K provided $f < 0.010$. This finding confirms that the model is stable when f ranges from 0 to 0.010. Since the perturbations employed are small, the stability proved is linear stability. To consider the nonlinear stability we need to look at how solutions evolve when perturbations far from the control climate are applied (Schneider, 1973).

If a nonlinear process is invoked, the system may have multiple equilibria. Indeed, it is well known that many time-independent EBMs have three (e.g. North, 1975) or even more (Ghil, 1976) steady-state solutions when the ice-albedo effect is included. To find out if our model also possesses this characteristic, we started the integration with initial conditions far away from the control climate. The model is found to be very stable to positive temperature perturbations. However, an additional solution besides the present climate appears if negative perturbations in the initial conditions are more than 20 K, provided $f > 0.005$. The second solution is characterised by very low temperatures everywhere, which will be referred to as an ice-covered earth solution. However, the ice-covered earth solution disappears for $f < 0.005$, no matter how strong the perturbation is. For $f < 0.005$, the model has only one unique solution which is the present climate. This state is very stable.

Finally we would like to show the diagnosed freshwater flux associated with the CO_2 doubling experiment in Fig. 5. We see that the freshwater flux is altered most significantly in middle latitudes, although there also appears a remarkable change near the equator. There is a general reduction of the flux within the latitude zone from 50° S to 40° N expect near the equator, whereas a significant increase can be observed near 55° S and 45° N. A similar AGCM experiment carried out by Manabe and Wetherald (1980) (hereafter referred to as MW) shows a decrease in the flux equatorward of about $40°\,^{N}_{S}$ and an increase polarward of about $40°\,^{N}_{S}$. The increase within the narrow latitude zone shown by version 1 is attributable to the most significant temperature change predicted there. As the atmospheric heat transport is fixed, the diffusion parameterization for the sensible heat transport implies that change in the latent heat transport is also linked to the meridional temperature gradient. Therefore, the most remarkable increase of temperature around $50°\,^{S}_{N}$ results in the increased freshwater flux mentioned above.

5.2 *Version 2*

The same perturbation is also added to version 2 of the model. The equilibrium response of the model to the perturbation with f ranging from 0.00 to 0.010 is shown in Fig. 6. Compared with the response in version 1, version 2 shows a much smoother change in the temperature with respect to latitude. Obviously this is due to the variable heat transport built in. While the great sensitivity in the vicinity of the ice line disappears, an evident polar amplifying effect is observed in Fig. 6. This effect is more evident as the ice-albedo factor f increases. Since the parameterization of the albedo is as the same as that in version 1, the polar amplifying effect found in version 2 may be

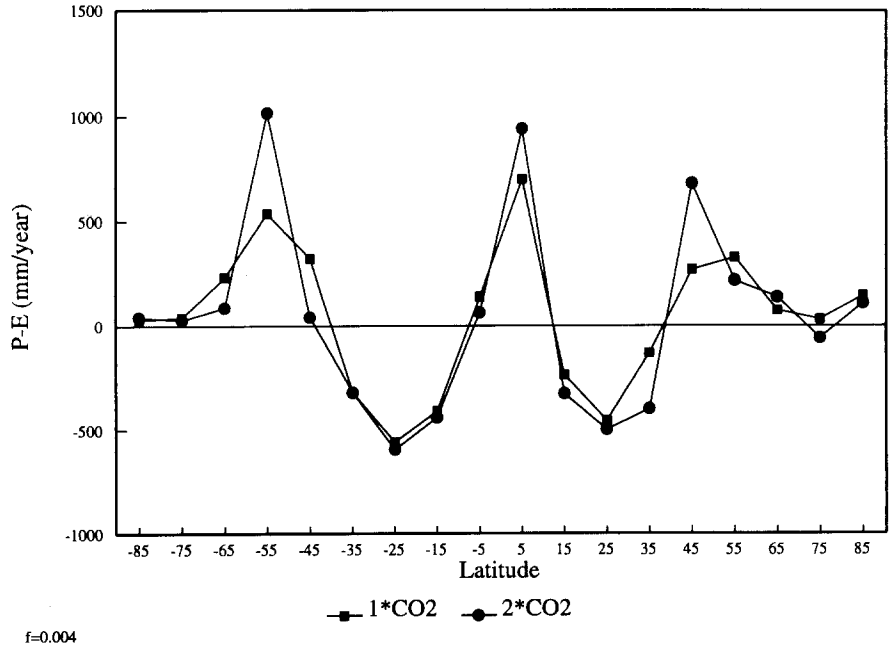

Fig. 5. Freshwater fluxes in the control climate and in the experiment with the doubling of the atmospheric CO_2

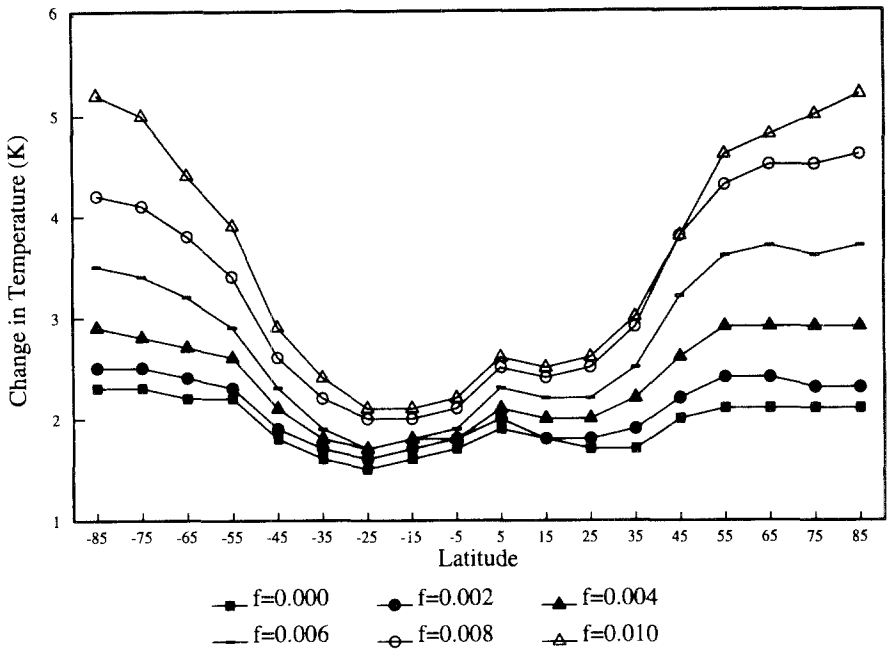

Fig. 6. Model responses to a doubling of CO_2 with different ice-albedo feedback factors. Temperature changes are expressed by the difference between the equilibrium temperature distribution due to the doubling of CO_2 and that of the control climate

attributed to an additional feedback mechanism: transport-temperature feedback.

The increases in the global mean temperature of version 2 are 1.8, 1.9, 2.1, 2.4, 2.8, 3.0 K for $f = 0.00$, 0.002, 0.004, 0.006, 0.008, 0.010 respectively. Although the local sensitivity of version 2 differs remarkedly from version 1, the global sensitivities of the two versions show good agreement. Version 2 shows a slightly smaller global sensitivity than version 1, indicating that the transport-temperature feedback is a negative feedback in this case. Version 2 produces a much smoother latitudinal temperature variation than version 1. The smoother temperature variation will not cause a problem for the diagnostics of the freshwater flux as in version 1. Contrary to the rather small value of f in version 1, we use $f = 0.006$ in version 2.

We also studied the possibility of multiple equilibria in version 2. It shows similar results as found with version 1. When $f \leqslant 0.006$ the ice-covered earth solution disappears.

Note that the only difference between the two versions is, in terms of the feedback analysis, that version 2 has one more mechanism operating. The effect of the feedback on the global sensitivity can be assessed by a feedback parameter λ_T. As discussed above, λ_T is simply the difference between the two total feedback parameters of the two versions with an equal λ_α. For $f = 0.006$ the total feedback parameter $\lambda_1 = \frac{4}{2.4}\frac{W}{m^2K}$ and $\lambda_2 = \frac{4}{2.7}\frac{W}{m^2K}$ for version 1 and 2, respectively. This results in an estimate of $\lambda_T = 0.19\,\mathrm{Wm^{-2}K^{-1}}$ for the total heat transport. From the experiments with version 1 we estimate $\lambda_\alpha = -0.74\,\mathrm{Wm^{-2}K^{-1}}$ for $f = 0.006$.

The polar amplifying effect in version 2 is very interesting because it reproduces an important feature of the global warming commonly found in AGCMs. This warming in AGCMs has been interpreted as due to positive lapse rate and ice-albedo feedbacks at high latitudes. However, the parameterization of heat transport associated with the ice-albedo feedback in our model appears to be responsible for the amplification. MW point out that increased latent heat transport in a warmer climate contributes to the reduction in meridional temperature gradient near the surface. In Fig. 7 the latent transports in response to the doubling of CO_2 and that from the control climate are shown. The latent heat transport increases at all latitudes in our model, which is due to the exponential temperature dependence of the saturation water vapour pressure with warming. The maximum increase appears near the equator, because $\partial q_{0s}/\partial T_0$ increases with increasing temperature. It is expected that the increased latent heat transort will result in an increase in amplitude of the freshwater flux. The diagnosed freshwater flux associated with the CO_2 doubling experiment and that from the control climate are displayed in Fig. 8. The freshwater supply to the

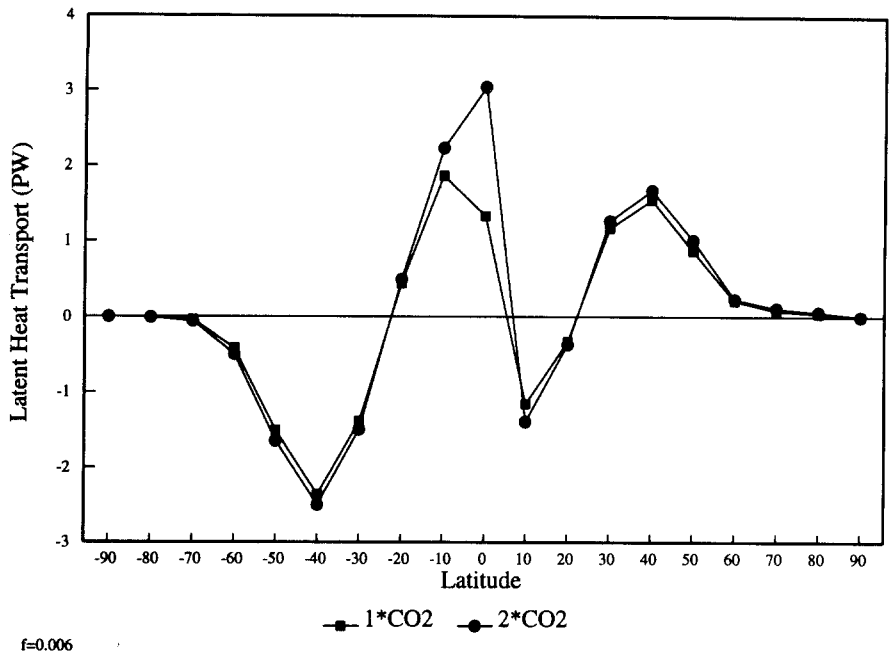

Fig. 7. Latent heat transports due to a doubling of the atmospheric CO_2 and that from the control climate

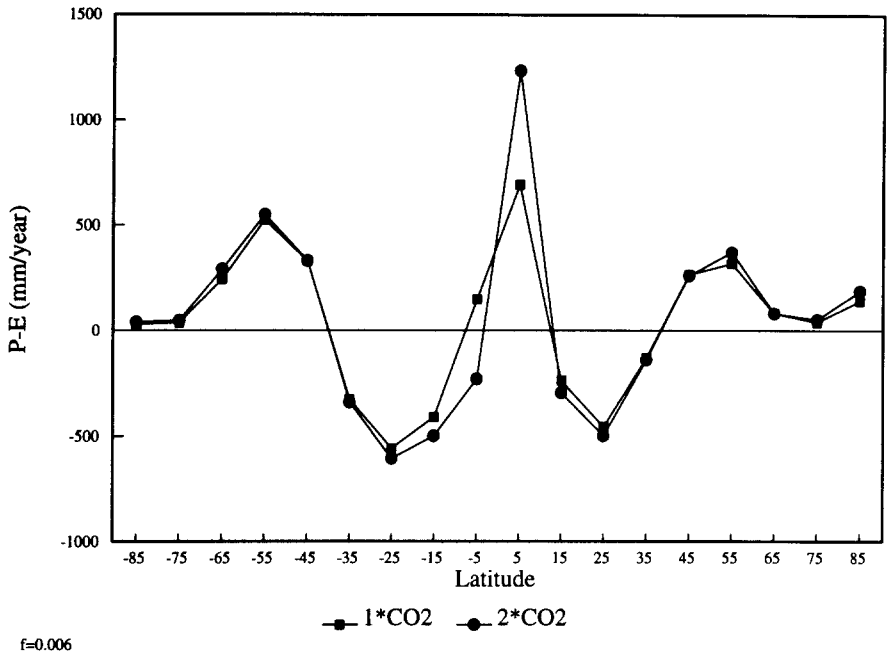

Fig. 8. Freshwater fluxes in the control climate and in the experiment with the doubling of the atmospheric CO_2

ocean will increase at middle and high latitudes and near the equator, whereas a general decrease is found at subtropical latitudes. This result is very similar to that of MW.

On the other side, as the meridional temperature gradient decreases in the warmer climate, the sensible heat transport which is proportional to the gradient will decrease. From Fig. 9 we can see that to a large extent the increased latent heat transport is compensated by the reduced sensible heat transport in our model, as is found in MW.

A closer examination shows that the atmospheric transport is reduced in the warmer climate almost everywhere with the maximum reduction around middle latitudes, though the changes are small. While the decrease at middle and high latitudes agree well with the results of MW, the decrease at low latitudes is just opposite to what is found by MW. The net increase at low latitudes found by MW is due to the fact that the amplitudes of the latent and sensible heat transports are almost equal in their model, implying that the

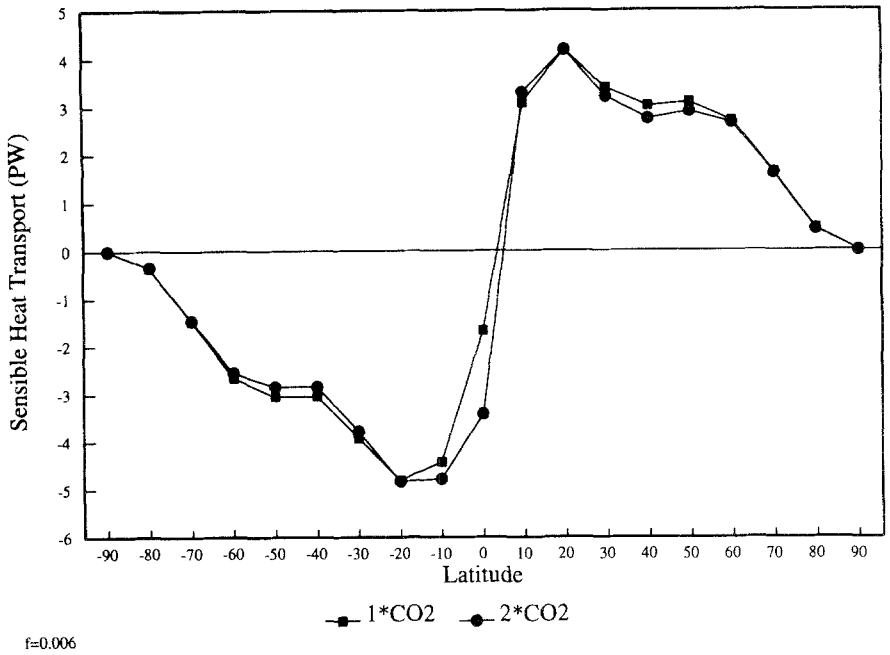

Fig. 9. Sensible heat transport in the control climate and in the experiment due to a doubling of the atmospheric CO_2

hydrological cycle in MW's model is very strong. In our model, however, the sensible heat transport is about three times larger than the latent transport. Therefore, the reduction in the sensible transport plays a dominant role, resulting in the decrease in the atmospheric transport. It is interesting to notice that version 2 predicts a larger increase in the temperature at high latitudes under the global warming even though the atmospheric heat transport is reduced. This result indicates that it is the combined effect of the ice-albedo and transport-temperature feedbacks that causes the polar amplification.

6. Conclusions

Based on the results of the experiments, following concluding remarks may be made:

1. Two distinct thermal inertias are found to be able to describe well the global atmosphere in the context of time dependent 1-D EBMs.
2. It appears that the largest uncertainty for the sensitivity of global mean temperature to perturbations is the magnitude of the ice-albedo feedback factor. On the other side, the parameterizations for the heat transport have great impact on local sensitivity.
3. The ice-albedo feedback not only strongly affects the sensitivity and stability of the model, but also controls the existence of multiple equilibrium solutions.
4. Although the experiments with version 2 show that the total heat transport under different forcings can be satisfactorily approximated as constant, the tiny variation of the transport does change the local responses significantly, especially those at middle and high latitudes, because of the ice-albedo feedback. Thus, the coupling between the transport and the feedback appears to be very important.
5. In terms of the predicted temperature and the diagnosed freshwater flux distribution, version 2 closely reproduces results from similar AGCM experiment. Hence, the application of version 2 will be preferred.
6. This EBM is appealing because of its simplicity to allow quick integrations and its ability to reproduce most important qualitative features of the climate variability found from AGCM simulations.

Although much work remains to be done before the extent to which this simple atmospheric model can help us in understanding the problems in ocean modelling can be assessed, we feel that the simple energy balance models have an important role to play in our developing knowledge of the coupling between the atmosphere and ocean. The EBM has been coupled to the OGCM. The

results of the interactive experiments will be reported elsewhere.

Acknowledgements

We wish to thank Prof. Dr. Dirk Olbers and Prof. Dr. Sven Lindqvist for their support of this work. This paper has AWI contribution number 894.

References

Budyko, M. I., 1969: The effect of solar radiation variations on the climate of the earth. *Tellus*, **21**, 611–619.

Bryan, F., 1986: High-latitude salinity effects and interhemispheric thermohaline circulations. *Nature*, **323**, 301–304.

Carissimo, B. C., Oort, A. H., Vonder Haar, T. H., 1985: Estimating the meridional energy transports in the atmosphere and ocean. *J. Phys. Oceanogr.*, **15**, 82–91.

Covey, C., 1988: Atmospheric and oceanic heat transport: simulations versus observations. *Climatic Change*, **13**, 149–159.

Dickinson, R. E., 1986: How will climate change? In: Bolin, B., Doos, B. R., Jaeger, J., Warrick, R. A. (eds.) *The Greenhouse Effect, Climate Change and Ecosystems*. SCOPE Rep., 29, pp. 206–270.

Ghil, M., 1976: Climate stability for a Sellers-type model. *J. Atmos. Sci.*, **33**, 3–20.

Haney, R. L., 1971: Surface thermal boundary conditions for ocean circu ation models. *J. Phys. Oceanogr.*, **1**, 241–248.

Harvey, L. D. D., 1988: A semianalytic energy balance climate model with explicit sea ice snow physics. *J. Climate*, **1**, 1065–1085.

Lal, M., Ramanathan, V., 1984: Effects of moist convection and water vapour radiative processes on climate sensitivity. *J. Atmos. Sci.*, **41**, 2238–2249.

Lashof, D. A., 1989: The dynamic greenhouse: Feedback processes that may influence future concentrations of atmospheric gases and climatic change. *Climatic Change*, **14**, 213–242.

Lian, M. S., Cess, R. D., 1977: Energy balance climate models: A reappraisal of ice-albedo feedback. *J. Atmos. Sci.*, **34**, 1058–1062.

Manabe, S., Bryan, K., 1985: CO_2-induced change in a coupled ocean-atmosphere model and its paleoclimatic implications. *J. Geophys. Res.*, **90**, 11,689–11,707.

Manabe, S., Wetherald, R. T., 1980: On the distribution of climate change resulting from an increase in the CO_2 content of the atmosphere. *J. Atmos. Sci.*, **37**, 99–118.

Mitchell, J. F. B., 1987: Climate sensitivity and past climates; Evidence from numerical studies. In: Berger, W. H., Labeyrie, L. D., (eds.) *Abrupt Climatic Change*. Hingham, Mass.: D. Reidel, pp. 383–398.

Mitchell, J. F. B., 1989: The "greenhouse" effect and climate change. *Rev. Geophys. Space Phys.*, **27**, 115–139.

North, G. R., 1975: Theory of energy-balance climate models. *J. Atmos. Sci.*, **32**, 2033–2043.

North, G. R., Cahalan, R. F., Coaley, J. A., 1981: Energy balance climate models. *Rev. Geophys. Space Phys.*, **19**, 91–121.

Oort, A. H., Rasmusson, E. M., 1970: On the annual variation of monthly mean meridional circulation. *Mon. Wea. Rev.*, **98**, 423–442.

Oort, A. H., Rasmusson, E. M., 1971: Atmospheric circulation statistics, NOAA Prof. Pap. No. 5, Govt. Printing Office, Washington, D. C., 323 pp.

Oort, A. H., 1983: Global atmospheric circulation statistics, 1958–1973. NOAA Prof. Pap. No. 14, Govt. Printing Office, Washington, D. C., 180 pp + microfiches.

Pacanowski, R., Dixon, K., Rosati, A., 1991: The G.F.D.L modulor ocean model user's guide version 1.0, GFDL Ocean Group Techn. Report #2.

Rennick, M. A., 1977: The parameterization of tropospheric lapse rates in terms of surface temperature. *J. Atmos. Sci.*, **34**, 854–862.

Roads, J. O., Vallis, G. K., 1984: An energy balance climate model with cloud feedbacks. *Tellus*, **36A**, 236–250.

Schneider, S. H., Gal-Chen, T., 1973: Numeric experiments in climate stability. *J. Geophys. Res.*, **78**, 6182–6194.

Sellers, W. D., 1969: A global climate model based on the energy balance of the earth-atmosphere system. *J. Appl. Meteor.*, **8**, 392–400.

Spelman, M. J., Manabe, S., 1984: Influence of oceanic heat transport upon the sensitivity of a model climate. *J. Geophys. Res.*, **89**, 571–586.

Stephens, G. L., Campbell, G..G., Vonder Haar, T. H., 1981: Earth radiation budgets. *J. Geophys. Res.*, **86**, 9739–9760.

Stocker, T. F., Wright, D. G., Mysak, L. A., 1992: A zonally averaged, coupled ocean-atmosphere model for paleoclimate studies. *J. Climate*, **5**, 773–797.

Taljaard, J., Loon, H. van, Crutcher, H. L., Jenne, R. L., 1969: Climate of the Upper Air: Southern Hemisphere, Vol. 1, Temperatures, Dewpoints, and Heights at Selected Pressure Levels. NAVAIR 50-1c-55, Chief Naval Operations, Washington D. C., 135 pp.

Washington, W. M., Meehl, G. A., 1983: General circulation model experiments on the climatic effects due to a doubling and quadrupling of carbon dioxide concentration. *J. Geophys. Res.*, **88**, 6600–6610.

Washington, W. M., Meehl, G. A., 1984: A seasonal cycle experiment on the climatic sensitivity due to a doubling of CO_2 with an atmospheric general circulation model coupled to a simple mixed layer ocean model. *J. Geophys. Res.*, **89**, 9475–9503.

Weaver, A. J., Marotzke, J., Cummins, P. F., Sarachik, E. S., 1993: Stability and variability of the thermohaline circulation. *J. Phys. Oceanogr.*, **23**, 39–60.

Zhang, S., Greatbatch, R. G., Lin, C. A., 1993: A reexamination of the polar halocline catastrophe and implications for coupled ocean-atmosphere modeling. *J. Phys. Oceanogr.*, **23**, 287–299.

Authors' addresses: Dr. D. Chen, Department of Physical Geography, Earth Sciences Centre, Göteborgs University, 413 81 Göteborg, Sweden; Dr. R. Gerdes and G. Lohmann, Alfred-Wegener-Institute for Polar and Marine Research, Sektion Physik II, Am Handelshafen 12, D-27570 Bremerhafen, Germany.